12th International Conference on Applications of Statistics and Probability in Civil Engineering, ICASP12
Vancouver, Canada, July 12-15, 2015

Evaluating Desktop Methods for Assessing Liquefaction-Induced Damage to Infrastructure for the Insurance Sector

Indranil Kongar
Research Engineer, Earthquake and People Interaction Centre, University College London, UK

Tiziana Rossetto
Professor, Earthquake and People Interaction Centre, University College London, UK

Sonia Giovinazzi
Senior Research Fellow, Dept. Civil Engineering, University of Canterbury, Christchurch, NZ

ABSTRACT: The current method used by insurance catastrophe models to account for liquefaction simply applies a factor to shaking-induced losses based on liquefaction susceptibility. There is a need for more sophisticated methods but they must be compatible with the data and resource constraints that insurers have to work with. This study compares five models: liquefaction potential index (LPI) calculated from shear-wave velocity; two implementations of the HAZUS software methodology; and two models based on USGS remote sensing data. Data from the September 2010 and February 2011 Canterbury (New Zealand) earthquakes is used to compare observed liquefaction occurrences to predictions from these models using binary classification performance measures. The analysis shows that the best performing model is LPI although the correlation with observations is only moderate and statistical techniques for binary classification models indicate that the model is biased towards positive predictions of liquefaction occurrence.

1. INTRODUCTION

The recent earthquakes in Haiti (2010), Canterbury, New Zealand (2010-11) and Tohoku, Japan (2011) highlighted the significance of liquefaction as a cascading effect of seismic events. The insurance sector was caught out by these events, with catastrophe models underestimating the extent and severity of liquefaction that occurred. A contributing factor was that the method used by some models to account for liquefaction is based on liquefaction susceptibility, which only considers surficial characteristics. Furthermore, losses arising from liquefaction are predicted by adding an amplifier to losses predicted by ground shaking (Drayton and Vernon, 2013). Consequently, significant liquefaction-induced losses will only be predicted if significant losses are already predicted from ground shaking, whereas it is known that liquefaction can be triggered at relatively low ground shaking intensities (Quigley et al., 2013). Therefore there is scope for the insurance sector to find more sophisticated methods to predict liquefaction. This is particularly important for assessing potential damage to critical infrastructure systems, which are more likely to be affected by liquefaction (Bird and Bommer, 2004) and can have significant impacts on indirect economic losses caused by business interruption.

There are three options that loss estimators can attempt in dealing with ground failure hazards (Bird and Bommer, 2004). They can ignore it; use a simplified method; or conduct a detailed geotechnical assessment. The first option will likely lead to underestimation of losses in earthquakes where liquefaction is a major hazard. The last option, detailed assessment, is appropriate for single-site risk analysis but is impractical for insurance loss

estimation purposes because of three constraints: limited accessed to detailed geotechnical data; lack of expertise in method application; and the geographic scale of the exercise which may make detailed assessment expensive and time-consuming.

The overall aim of this research is to produce a methodology for assessing liquefaction hazard, which abides by these constraints and this paper focuses on one aspects of that research: the evaluation of existing methods for desktop liquefaction prediction.

2. LIQUEFACTION ASSESSMENT MODELS

There are two steps in the prediction of liquefaction occurrence (Bird et al., 2006). First it is necessary to determine whether soils are susceptible to liquefaction, based solely on ground conditions with no earthquake-specific information. This is often done qualitatively and sometimes, as currently the case with catastrophe models (Drayton and Vernon, 2013), this is also the full extent of liquefaction hazard that is considered. The next step is to determine liquefaction triggering, which extends the liquefaction susceptibility to determine earthquake-specific likelihood of liquefaction, based on earthquake parameters.

2.1. Liquefaction Potential Index

The most common approach used to predict liquefaction triggering is the factor of safety against liquefaction, *FS*. This can be defined as the ratio of the cyclic resistance ratio, *CRR*, and the cyclic stress ratio, *CSR*, for a layer of soil at depth, *z*. *CSR* can be expressed by:

$$CSR = 0.65\left(\frac{a_{max}}{g}\right)\left(\frac{\sigma_v}{\sigma_v'}\right)r_d \qquad (1)$$

where a_{max} is the peak horizontal ground acceleration; g is the acceleration of gravity; σ_v is the total overburden stress at given depth; σ_v' is the effective overburden stress at depth, *z*; and r_d is a shear stress reduction coefficient dependent on depth. *CRR* is usually calculated from geotechnical parameters from cone penetration test or standard penetration tests. Andrus and Stokoe (2000) proposed an alternative method for calculating CRR based on shear-wave velocity, V_s, in which:

$$CRR = \left\{ \begin{matrix} 0.022\left(\frac{V_{S1}}{100}\right)^2 + \\ 2.8\left(\frac{1}{V_{S1}^* - V_{S1}} - \frac{1}{V_{S1}^*}\right) \end{matrix} \right\} MSF \qquad (2)$$

where V_{S1} is the stress-corrected shear wave velocity; V_{S1}^* is the limiting upper value of V_{S1} for cyclic liquefaction occurrence, and *MSF* is a magnitude scaling factor. The equations for V_{S1} and *MSF* are not repeated here.

Liquefaction is predicted to occur when $FS \leq 1$ and predicted not to occur when $FS > 1$. However Juang et al. (2005) found that the CRR model is conservative, resulting in lower factors of safety and over-prediction of liquefaction occurrence. To correct for this, Juang et al. (2005) propose a multiplication factor of 1.4 to obtain an unbiased estimate of the factor of safety, $FS^* = 1.4 \times FS$.

FS^* is an indicator of potential liquefaction at a specific depth, i.e. for a single soil layer, however Iwasaki et al. (1984) noted that damage to structures due to liquefaction was affected by liquefaction severity. They proposed an extension to this approach – the liquefaction potential index, *LPI*, to predict the likelihood of surface-level manifestation of liquefaction based on integrating a function of the factors of safety across the top 20m of soil. *LPI* is calculated from:

$$LPI = \int_0^{20} F^*(10 - 0.5z)dz \qquad (3)$$

where $F^* = 1 - FS^*$ for a particular soil layer and the inclusion of the depth function ensures greater weighting is given to factors of safety closer to the surface. The original guidance criteria from Iwasaki et al. (1984) proposes that the potential for liquefaction was very low for $LPI = 0$; low for $0 < LPI \leq 5$; high for $5 < LPI \leq 15$; and very high for $LPI > 15$. With respect to its usefulness to the insurance sector, there are limitations to this methodology. In order to determine the overburden stresses, it is necessary

to know or estimate the water table depth and the soil unit weights both above and below the water table. Furthermore, while the use of *Vs* to calculate *CRR* negates the requirement for ground investigation, *Vs* data is not necessarily readily available at many locations.

2.2. HAZUS

HAZUS®MH MR4 (NIBS, 2003) is a loss estimation software package for the United States and includes a module for predicting the probability of liquefaction. The first step is to determine zones of liquefaction susceptibility from an existing map or from surficial geology. Both of these approaches may pose problems for insurers since surface geology maps are not widely and freely available to non-academic organizations and even where existing maps are available, the zone characteristics may not translate directly. For a given liquefaction susceptibility zone, the probability of liquefaction occurrence is given by:

$$P[Liq] = \frac{P[Liq|PGA=a]}{K_M K_w} P_{ml} \qquad (4)$$

where $P[Liq|PGA=a]$ is the conditional probability of liquefaction occurrence for a given susceptibility zone at a specified level of peak horizontal ground motion, a; K_M is the moment magnitude correction factor; K_w is the ground water correction factor; and P_{ml} is the proportion of map unit susceptible to liquefaction, which accounts for the real variation in susceptibility across similar geologic units. The equations for calculating these factors are not repeated here. In addition to the problems in determining liquefaction susceptibility zones, the HAZUS method also requires the water table depth to be known or estimated.

2.3. *Zhu et al. (2014)*

Zhu et al. (2014) have developed empirical functions to predict liquefaction probability specifically for use in rapid response and loss estimation. They deliberately use predictor variables that are quickly and easily accessible and do not require specialist knowledge to apply. For a given set of predictor variables, the probability of liquefaction is then given by the logit link function:

$$P[Liq] = \frac{1}{1+e^{-X}} \qquad (5)$$

Two linear models for X are proposed in their paper: a regional model for use in coastal sedimentary basins and a global model that is applicable more generally. The functions are not repeated here, but in the global model X is dependent on $PGA_{M,\mathrm{SM}}$, which is the product of the peak horizontal ground acceleration from ShakeMap estimates (USGS, 2014a) and a magnitude weighting factor; V_{s30}, the average shear wave velocity to 30m depth from the USGS Global Map Server (USGS, 2013); and *CTI*, which is the compound topographic index, used as a proxy for saturation, and which can be obtained globally from the USGS Earth Explorer web service (USGS, 2014b). The regional model uses the same parameters and additionally *ND*, which is the distance to the coast, normalized by the size of the sedimentary basin, which is determined from surface roughness. This method is advantageous over *LPI* and HAZUS as it does not require knowledge of water table depth or soil weight.

3. MODEL TEST APPLICATION

3.1. Observed data

The models are tested by comparing site specific predictions to liquefaction observations from the M_w 7.1 and M_w 6.2 earthquakes that struck Christchurch, New Zealand on September 4th 2010 and February 22nd 2011 respectively. This study considers binary observations of liquefaction occurrence based on ground investigation data provided by Tonkin & Taylor (geotechnical consultants to the New Zealand Earthquake Commission) and maps from the Canterbury Geotechnical Database (CGD, 2013a). It is important to note that these observations account for surface manifestations of liquefaction only and so may under-represent the true extent of liquefaction, although it is sufficient for this study given that *LPI* is

developed to predict surface liquefaction and the HAZUS prediction model only considers surface characteristics in its assessment.

3.2. Prediction model inputs

For the *LPI* model, V_s profiles for 13 sites across the city (Wood et al., 2011) are used and ordinary kriging is applied between points to create V_s surfaces at 1m intervals to a depth of 20m. A water table depth of 2m is assumed across Christchurch, reflecting the averages described by Giovinazzi et al. (2011) and soil unit weights of 17kPa above the water table and 19.5kPa below the water table are assumed. Whilst Andrus and Stokoe (2000) advise that the maximum V_{s1} can range from 200-215m/s depending on fines content, subsequent work by Zhou and Chen (2007) indicates that the maximum V_{s1} could range between 200-230m/s. In the absence of specific fines content data, a median value of 215m/s is assumed to be the maximum.

Because of the regional scale of this analysis, site-specific soil profile is not taken into account in determining whether layers are liquefiable. Borehole data at sites close to the V_s profile sites are available from the Canterbury Geotechnical Database (CGD, 2013b). These indicate that in the eastern part of Christchurch, soil typically consists predominantly of clean sand to 20m depth, with some layers of silty sand. In the western parts of Christchurch however there is an increasing mix of sand, silt and gravel in soil profiles, particularly at depths down to 10m. Therefore it is possible, particularly in western suburbs, that calculated V_{s1} values may indicate liquefiable soil layers when the soil type is not appropriate, which would consequently lead to overestimation of liquefaction potential. The *PGA* 'shakefield' for the *LPI* model is taken from the Canterbury Geotechnical Database (CGD, 2013c).

For application of the HAZUS method, liquefaction susceptibility zones are determined from the liquefaction susceptibility map for Canterbury (ECan, 2014), from which it is possible to identify four susceptibility categories: None, Low, Moderate and High. Since these need to be translated into the six susceptibility categories defined by HAZUS, two implementations of the HAZUS method are used in this study. In both implementations, the 'None' and 'Moderate' categories translate directly. In the first implementation, the 'Low' and 'High' categories also translate directly, but in the second, 'Low' on the map translates to 'Very low' in HAZUS, and 'High' from the map translates to 'Very high' in HAZUS.

Both the global and regional models proposed by Zhu et al. (2014) are tested. The *PGA* 'shakefield' from the Canterbury Geotechnical Database (CGD, 2013c) is used as an equivalent to the USGS ShakeMap, whilst *CTI*, *Vs30* and the DEM to calculate *ND*, have been acquired from the relevant USGS web resources. In total five models are tested, based on three general methodologies, as described in Table 1.

Table 1: Liquefaction prediction methods being tested

Model	Description
LPI1	*LPI* with V_S profiles
HAZ1	HAZUS with direct translation from liquefaction susceptibility map
HAZ2	HAZUS with modified translation from liquefaction susceptibility map
ZHU1	Global model by Zhu et al. (2014)
ZHU2	Regional model by Zhu et al. (2014)

3.3. Test area

To ensure equivalence in the test, all methods are applied to the same test area, which is the region in which input data for all models is obtainable, whether directly or by geostatistical estimation. The test area is divided into a 100m x 100m grid, generating 25,100 grid blocks. Each block is attributed a classification based on observed liquefaction and a series of values representing the input parameters needed for the range of liquefaction prediction methods. From these, *LPI* and four liquefaction probabilities are calculated

for each block, creating five sets of site-specific assessment indices.

3.4. Site-specific prediction

When using semi-probabilistic prediction frameworks, one can interpret the calculated probability as a regional parameter that describes the spatial extent of liquefaction rather than discrete site specific predictions, and indeed Zhu et al. (2014) specifically suggest that this is how their model should be interpreted. So for example, one would expect 30% of all sites with a liquefaction probability of 0.3 to exhibit liquefaction and 50% of all sites with a probability of 0.5 etc. However, when using liquefaction predictions to estimate structural damage over a wide area, it is useful to know not just how much liquefaction is predicted to occur but also where. This is particularly important for infrastructure systems since the complexity of these networks means that damage to two identical components can have significantly different impacts on overall systemic performance depending on service areas and system redundancy.

One approach to generate site-specific predictions from probabilities is to group sites together based on their probability, and then randomly assign liquefaction occurrence to sites within the group to correspond to the probability. This method is good for ensuring that the spatial extent of the site specific predictions reflect the probabilities, but since the locations are selected randomly it has limited value for comparison of predictions to real observations.

Another method is to set a threshold value for liquefaction occurrence, so that only sites with a probability above the threshold are predicted to exhibit liquefaction. The disadvantage of this approach is that the resulting predictions may not reflect the original probabilities if the number of sites above and below the threshold are not proportionally distributed. However since there is no random element to the determination of liquefaction occurrence, the predictions are more definitive and hence more useful for the model testing in this study. No guidance is given for thresholds in HAZUS, whilst Zhu et al. (2014) propose a threshold of 0.3 to preserve spatial extent, although they also consider thresholds of 0.1 and 0.2. Thresholds can also be used to assign liquefaction occurrence based on *LPI* and Toprak and Holzer (2003) found that surface manifestation of liquefaction is unlikely for *LPI* < 5. Goda et al. (2011) note that this threshold for *LPI* is only appropriate if the bias-correction factor of Juang et al. (2005) is adopted in the *LPI* calculations.

4. MODEL TEST RESULTS

Comparison of binary classification predictions with observations is performed by summarizing data into 2 x 2 contingency tables for each model, identifying the quantity of true positives (*TP*), true negatives (*TN*), false positives (*FP*, Type I error) and false negatives (*FN*, Type II error) amongst the predictions. The true positive rate (*TPR* or sensitivity) is the ratio of *TP* to observed positives. The true negative rate (*TNR* or specificity) is the ratio of *TN* to observed negatives. The false positive rate (*FPR* or fall-out) is the ratio of *FP* to *TN*. An initial set of results using 5 as a threshold for LPI1, 0.3 as a threshold for the ZHU models and 0.5 as a threshold value for the HAZ models is shown in Table 2.

Table 2: Initial diagnostic scores for all liquefaction models

Method	*TPR*	*TNR*	*FPR*
LPI1	0.811	0.731	0.269
HAZ1	0.002	1.000	0.000
HAZ2	0.035	1.000	0.000
ZHU1	0.240	0.953	0.047
ZHU2	0.401	0.909	0.091

An ideal model would have a high *TPR* and *TNR* (> 0.5) and low *FPR* (< 0.5). The LPI1 model is the only model that meets these criteria. The small discrepancy between the *TPR* and *TNR* rates indicates some bias towards positive predictions, i.e. some ‘over-prediction’ of

liquefaction. This could be explained by the non-inclusion of site-specific soil profiles in *LPI* calculations. The high *TNR* and low *TPR* of the other models indicate a strong bias towards negative predictions of liquefaction. In the case of the two HAZ models this bias is extreme and in fact suggests that they nearly always predict non-liquefaction. However it is possible for these models that the extreme scores are due the threshold chosen.

For a single model, the receiver operating characteristic (ROC) curve is a plot of *TPR* on the y-axis against *FPR* on the x-axis for a range of threshold values. The ROC curves for each model are shown in Figure 1 where the 'chance line' (*TPR* = *FPR*) is equivalent to random guessing.

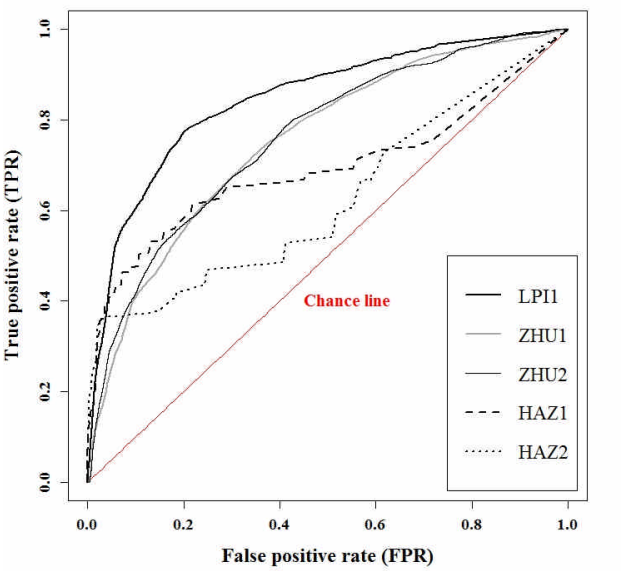

Figure 1: ROC curves for all liquefaction prediction models

A good model has a ROC above and to the left of the diagonal, with perfect classification occurring at (0,1). Since better models have points towards the top left of the plot, the area under the ROC curve, *AUC*, is a generalized measure of model quality that assumes no specific threshold. ROC curves for the five models and corresponding *AUC* values are generated using the ROCR package in R (Sing et al., 2005) and the results are shown in Table 3.

Since the diagonal is equivalent to random guessing, *AUC* = 0.5 suggests a model has no value, while *AUC* = 1 is a perfect model. It can be seen that the two HAZ models have *AUC*s closest to the 'no value' criterion, suggesting that the issue with these models may not just the threshold, but rather that they fundamentally under-predict liquefaction when used as implemented in this study. The only reason they are to the left of the chance line is that because they are making negative predictions at nearly every site, they are guaranteed to generate a low *FPR* value. The two ZHU models are an improvement on the HAZ models but there is little difference between them. As expected based on the data from Table 2, the LPI model is the best performing over the chance line.

The performance of the models can be further optimized by testing alternative thresholds. For a single ROC point, Youden's *J*-statistic is the height between the point and the chance line. When measured for every point on the ROC curve, the point which maximizes the *J*-statistic is representative of the optimal threshold. The optimum thresholds and corresponding *J*-statistics for each model are shown in Table 3. For the ZHU and HAZ models, the optimization is subject to a minimum threshold probability of 0.1.

Table 3: Statistics related to ROC curves for all liquefaction models

Method	*AUC*	Threshold	*J*-statistic
LPI1	0.845	7	0.573
HAZ1	0.691	0.1	0.261
HAZ2	0.623	0.1	0.314
ZHU1	0.753	0.1	0.355
ZHU2	0.760	0.1	0.371

The model with the largest *J*-statistic, i.e. the model that offers the greatest improvement over random guessing, is LPI1 with a threshold of 7. For *LPI*, Toprak and Holzer (2003) and Maurer et al. (2014) suggest triggering thresholds of 4

and 5 respectively. The optimum threshold of 7 for model LPI1 indicates that the methodology is predicting slightly high values for *LPI*, even with the bias correction. The likely cause of this is that site-specific soil profiles have not been taken into account and so layers that are not liquefiable are being mis-classified and contributing to higher *LPI* values. For the ZHU models and HAZ models, the optimum threshold is a probability of 0.1 based on the minimum constraint. This further indicates that these models may strongly underestimate liquefaction occurrence.

Based on all the scores used – *TPR*, *TNR*, *FPR*, *AUC* and Youden's *J*-statistic – the LPI1 model performs favorably over other desktop methods. As well as comparing to other desktop models however, it is also useful to measure the quality of the LPI1 model in its own right. The Matthews correlation coefficient, *MCC*, is related to the chi-squared statistic for a 2 x 2 contingency table and its interpretation is similar to Pearson's correlation coefficient. As such it can be treated as a measure of the goodness-of-fit of a binary classification model. The *MCC* value for the LPI1 model is 0.480 so it shows only a moderate correlation with the observations.

5. CONCLUSIONS

This study compares a range of simplified desktop liquefaction assessment methods that may be suitable for insurance sector where data availability and resources are key constraints. It finds that the model based on *LPI* calculated from V_s profiles performs favorably over other methods based on statistical measures of binary classification, although it is better at correctly predicting the occurrence of liquefaction than non-occurrence and so may over-predict overall. A possible explanation for the over-prediction is that soil profiles have not been taken into account and so layers may be misclassified as being liquefiable. An important consideration with soil profiles though is that loss estimators may not have access to this data and where it is available it is not necessarily feasible to include in a regional scale model. The use of typical soil profiles (e.g. Goda et al., 2011) is a useful compromise to reduce but not necessarily eliminate the over-prediction problem. There is some correlation between the observed data and model predictions with this *LPI* methodology. Although it is not strong, it may be considered acceptable by loss estimators when considering the simplifications that are necessary to meet the constraints imposed by regional scale catastrophe modeling.

The HAZUS methodology for estimating liquefaction probabilities performs poorly irrespective of triggering threshold. This is significant since HAZUS methodologies are often used as a default model outside of the US when no more locally (or regionally) specific model is available. The two models proposed by Zhu et al. (2014) perform better than HAZUS, but not as well as *LPI*, and show a negative prediction bias. It is important to note that their models have been developed for prediction of liquefaction extent, not site-specific predictions so this result is not surprising. Given that data input requirements for the Zhu models are more straightforward than for the *LPI* model, they may still have potential for site-specific prediction of liquefaction within insurance sector if the bias can be accounted for.

There are four pieces of work that would be useful for building on and improving on this study. The first is to repeat the analysis for other events to see if the models produce similar scores when applied elsewhere. The second is to test to what extent the use of these methods would have improved loss estimates for real case studies such as Christchurch. The third is to use observed data to develop new liquefaction prediction models or adapt existing ones. Finally, the study can be extended to test the accuracy of models that predict measurements of the permanent ground deformation.

6. ACKNOWLEDGMENTS

This research has been funded by the Willis Research Network and the UK Engineering and Physical Sciences Research Council through the Urban Sustainability and Resilience program at

University College London. The authors acknowledge the support of Sjoerd van Ballegooy at Tonkin & Taylor for provision of Christchurch ground investigation GIS data.

7. REFERENCES

Andrus, R. D. and Stokoe, K. H. (2000). "Liquefaction resistance of soils from shear-wave velocity." *J. Geotech. Geoenviron.*, 126(11), 1015-1025.

Bird, J. F. and Bommer, J. J. (2004). "Earthquake losses due to ground failure." *Eng. Geol.*, 75, 147-179.

Bird, J. F., Bommer, J. J., Crowley, H. and Pinho, R. (2006). "Modelling liquefaction-induced building damage in earthquake loss estimation." *Soil Dyn. Earthq. Eng.*, 26, 15-30.

CGD. (2013a). *Liquefaction and Lateral Spreading Observations – Map Layer CGD0300*, https://canterburygeotechnicaldatabase.projectorbit.com/.

CGD. (2013b). *Geotechnical Investigation Data – Map Layer CGD0010*, https://canterburygeotechnicaldatabase.projectorbit.com/.

CGD. (2013c). *Conditional PGA for Liquefaction Assessment – Map Layer CGD5110 – 21 Feb 2013*, https://canterburygeotechnicaldatabase.projectorbit.com/.

Drayton, M. J. and Verdon, C. L. (2013). "Consequences of the Canterbury earthquake sequence for insurance loss modelling." *Proc. 2013 NZSEE Conf.*, NZSEE, Wellington, NZ.

ECan. (2014). "OpenData Portal." *Canterbury Maps*, http://opendata.canterburymaps.govt.nz/

Giovinazzi, S., Wilson, T., Davis, C., Bristow, D., Gallagher, M., Schofield, A., Villemure, M., Eidinger, J. and Tang, A. (2011). "Lifelines performance and management following the 22nd February 2011 Christchurch earthquake, New Zealand: highlights of resilience." *B. NZ. Soc. Earthq. Eng.*, 44(4), 402-417.

Goda, K., Atkinson, G.M., Hunter, A.J., Crow, H. and Motazedian, D. (2011). "Probabilistic liquefaction hazard analysis for four Canadian cities." *Bull. Seismol. Soc. Am.*, 101(1), 190-201.

Iwasaki, T., Arakawa, T. and Tokida, K.-I. (1984). "Simplified procedures for assessing soil liquefaction during earthquakes." *Soil Dyn. Earthq. Eng.*, 3(1), 49-58.

Juang, C.H., Yang, S.H. and Yuan, H. (2005). "Model uncertainty of shear wave velocity-based method for liquefaction potential evaluation." *J. Geotech. Geoenviron.*, 131(10), 1274-1282.

Maurer, B. W., Green, R. A., Cubrinovski, M. and Bradley, B. A. (2014). "Evaluation of the liquefaction potential index for assessing liquefaction potential in Christchurch, New Zealand." *J. Geotech. Geoenviron.*, 140(7), 04014032.

NIBS. (2003). *HAZUS®MH Technical Manual*, Washington, D.C.

Quigley, M., Bastin, S. and Bradley, B. A. (2013). "Recurrent liquefaction in Christchurch, New Zealand, during the Canterbury earthquake sequence." *Geology*, 41(4), 419-422.

Sing, T., Sander, O., Beerenwinkel, N. and Lengauer, T. (2005). "ROCR: visualizing classifier performance in R." *Bioinformatics*, 21(20), 3940-3941.

Toprak, S. and Holzer, T. L. (2003). "Liquefaction potential index: field assessment." *J. Geotech. Geoenviron.*, 129(4), 315-322.

USGS. (2013). "Global V_S^{30} map server." *Earthquake Hazards Program*, http://earthquake.usgs.gov/hazards/apps/vs30/

USGS. (2014a). "ShakeMaps." *Earthquake Hazards Program*, http://earthquake.usgs.gov/earthquakes/shakemap/

USGS. (2014b). *Earth Explorer*, http://earthexplorer.usgs.gov/

Wood, C., Cox, B. R., Wotherspoon, L., and Green, R. A. (2011). "Dynamic site characterization of Christchurch strong motion stations." *B. NZ Soc. Earthq. Eng.*, 44(4), 195-204.

Zhou, Y.-G. and Chen, Y.-M. (2007). "Laboratory investigation on assessing liquefaction resistance of sandy soils by shear wave velocity." *J. Geotech. Geoenviron.*, 133, 959-972.

Zhu, J., Daley, D., Baise, L. G., Thompson, E. M., Wald, D. J., Knudsen, K. L. (2014). "A geospatial liquefaction model for rapid response and loss estimation." *Earthq. Spectra*, in press.